iJRASET
International Journal For Research in
Applied Science and Engineering Technology

INTERNATIONAL JOURNAL FOR RESEARCH
IN APPLIED SCIENCE & ENGINEERING TECHNOLOGY

Volume: 9 Issue: IX Month of publication: September 2021

DOI: https://doi.org/10.22214/ijraset.2021.37959

www.ijraset.com

Call: 08813907089 | E-mail ID: ijraset@gmail.com

# Integration of Geological, Geochemical, Mineralogical and Remote Sensing Data for Studying Zeolite Deposits of Al-Ahyuq-Taiz, Yemen

Ali M. Qaid[1], Ali M. Al-Hawbani[2], Naji Alqubati[3]
[1]Dep. of Civil Engineering technology, Al-Hajar (Qabitah) Community College / Lahj
[2]Dep. of Geology & Environmental Sciences, Faculty of Applied Sciences, Thamar University, Yemen
[3]Geological Survey and Mineral Resources Board, Sana'a

***Abstract: Zeolite deposits crop out at Al-Ahyuq area, and lies at about 89 km southwest of Taiz city. It is one of the most important zeolite localities in Yemen. The study area is covered by the Yemen volcanic group. X-Ray Diffraction (XRD) analyses showed that clinoptilolite is the major type of Al-Ahyuq zeolites with high purity. Chemical analysis shows that the studied zeolitic tuff samples have silica content ranging from 63.10 wt% - 71.1wt% with an average 68.69 wt%, $Fe_2O_3$ [as total iron] with an average 2.38wt%, MgO with an average 0.44 wt% and $TiO_2$ with an average 0.17wt%. These chemical properties of Al-Ahyuq zeolite deposits are with low impurities content such as CaO and MgO, compared to those deposits found in other countries around the world. The chemical and mineralogical studies support that the zeolite minerals of the Al-Ahyuq area formed by subaerial hydrothermal alteration of the parent volcanic glass. The ASTER bands as false colour composite (1-R, 2-G, 3-B), and band ratios 3/9 and 4/6 highlighted area of zeolite deposits dominated as bright pixels. The band ratio combination 4/6-R, 2/1-G and 3/2-B is effective in mapping of Al-Ahyuq zeolitic tuffs. Spectra after being resampled to ASTER VNIR+SWIR bands of the study area comparing with the USGS library spectra of zeolite – clinoptilolite shows almost identical and confirmed that clinoptilolite is the major of zeolite deposits in Al-Ahyuq area. Chemical and mineralogical investigation of the Al-Ahyuq zeolite (clinoptilolite) deposits recommends many important agricultural, environmental, and industrial applications.***
***Keyword: Zeolitic tuff; clinoptilolite; XDR; XRFS; ASTER data; band ratio***

## I. INTRODUCTION

The study area is bounded by the UTM coordinates 365400 and 363900 E and from 1450150 to 1452550 N (Fig. 1). It is covered by Yemen volcanic group which consists of two subunits of basalt at the bottoms, and zeolitic tuffs and rhyolites at the top. A promising source of economic growth is industrial mineral resources. Zeolitic deposits are one of the important industrial minerals in Yemen, and a potential key factor in the development of the economy. Zeolites are natural porous minerals of volcanic origin described as crystalline, hydrated aluminosilicates with exchangeable cation [1]–[4]. They consist of infinitely extended three-dimensional networks of $SiO_4^{-4}$ and $AlO_4^{-5}$ tetrahedra linked by shared oxygen atoms [5]–[8]. Natural zeolites are minerals formed at low temperatures and consists of a group of very open crystalline silicate minerals [9]–[12]. Zeolites have special and extraordinary physical and chemical properties that make them very useful in a wide range of applications, including agronomy, ecology, certain manufacturing, industrial processes, medicine, and cosmetics [13]. They are characterized by the ability of lose and gain water reversibly and to exchange extra-framework cations, both without altering the crystalline structure [14], [15].

The Cation Exchange Capacity (CEC) is essentially a function of the degree of aluminum substitution with silicon in the framework structure. The use of zeolites in different fields of science and practice is based on their ion exchange properties, which are one of the main parameters that characterize their sorption and technological properties [3]. Zeolites are used to dry gases separate oxygen from air, remove $NH_4^+$ from drinking water and wastewater, extract cesium (Cs) and strontium (Sr) from nuclear wastes [16] [17] [18]–[20]. Zeolites are used to remove heavy metals from agricultural and industrial wastewaters and to purify harmful emissions [21]–[24]. Natural zeolites have CECs from 2 to 4 meq/ g, about twice the CEC of bentonite clay. It has a relatively small CEC around 2.25 meq/g, but its cation selectivity is: Cs> Rb> K> NH4> Ba> Sr> Na> Ca> Fe> Al> Mg>Li [14]. The value for Clinoptilolite-rich tuffs ranging between 1.2 and 2 meq/g [15].

Zeolites in agriculture improve the efficiency of used fertilizers, thus promotes better plant growth and therefore enhances the yield [25]–[27], by taking up ammonia from animal manures, as dietary supplements to improve cation-exchange capacity and water sorption capacity [11], [28].

Another important aspect of the utilization of the zeolites is that they promote seeds germination [20], [29]–[31]. Zeolite is consistently used in diets for poultry, cattle and fish, improves grain weight and increases feed conversion rates [25], [32]. Zeolites have been used as a feed additive to improve the performance of poultry for layers and broilers, to assist in the management of manure and litter, and to positively influence the consistency of feces, to reduce diarrhea [9], [10], [24], [33], [34]. [5], suggested that zeolite could increase digestibility of feed as well as performance of broilers. Natural zeolites could be used in both human and veterinary medicine as biological active food additives (dietetic additives), drugs, drug carriers, anticancer adjuvants and antimicrobial agents [35], [36]. Zeolites appear to have been successful in the treatment of certain different human diseases, particularly in gastroenterology [36] and in removal of urea from the blood of patients with uremia [4], [35]–[39]. Clinoptilolite is one of the most abundant zeolites and is widely used in various applications, and according to International Mineralogical Association the nomenclature clinoptilolite has Si/Al> 4 [8], [16]. The thermal stability of the natural zeolite is directly proportional to the Si/Al ratio.

Remote sensing satellite imagery has high potential to provide a solution to overcome the problems and limitations associated with geological field mapping and mineral exploration. Advanced Spaceborne Thermal Emission and Reflection Radiometer (ASTER) is a multiband optical scanner on board NASA’s TERRA platform that was launched in December 1999. ASTER was designed by NASA and Japan's Ministry of Economy Trade and Industry (METI) as a next generation remote sensing sensor for earth observation following Landsat and JERS-1. ASTER provides optical data in 14 spectral bands: 3 bands from the visible to near infrared (VNIR), 6 bands from the shortwave infrared (SWIR) and 5 bands from the thermal infrared (TIR) wavelength regions (Table 1). ASTER data have shown success in application of remote sensing satellite imagery for mineral exploration and mapping of lithological units due to a higher spectral resolution in the short-wave infrared (SWIR) and thermal infrared (TIR) [40]–[43]. According to [44], the integral data of ASTER, field observation and mineralogical studies are useful for distinguishing and identifying natural zeolite (pure clinoptilolite-type) in volcano sedimentary in arid to semi-arid areas.

Table 1: Aster Data Band Ranges and Spatial Resolution

| Subsystem band | Band | Spectral range (μm) | Spatial resolution (m) |
|---|---|---|---|
| VNIR | 1 | 0.52–0.60 | 15 |
| | 2 | 0.63–0.69 | |
| | 3N | 0.76–0.86 | |
| | 3B | 0.76–0.86 | |
| SWIR | 4 | 1.60–1.70 | 30 |
| | 5 | 2.145–2.185 | |
| | 6 | 2.185–2.225 | |
| | 7 | 2.235–2.285 | |
| | 8 | 2.295–2.365 | |
| | 9 | 2.36–2.43 | |
| TIR | 10 | 8.125–8.475 | 90 |
| | 11 | 8.475–8.825 | |
| | 12 | 8.925–9.275 | |
| | 13 | 10.25–10.95 | |
| | 14 | 10.95–11.65 | |

Band ratio is a powerful technique in remote sensing, which prepared by dividing the DN of one band by the corresponding DN in another band for each pixel and displaying the new DN values as gray scale image [45]–[48]. It highlights the spectral difference between materials and reduces the variable effects of solar illumination and topography. Spectral characters of the surface materials analyzed and their abundance relative to the surrounding features of the surface are used for deciding the bands to be used in the band ratio images [49] [50][51] [52]. Ratio images can be combined to produce a colour image of any three monochromatic ratio datasets as G-R-B [45], [46], [53]: this technique widely used in mineral exploration, provides more geological information and shows greater contrast between rock units from as many bands in a single image and is very easy to visually interpret. Figure 1 shows the world production of natural zeolites in 2020 which is estimated at 1.1 million metric tons (Mt) [54].

ISSN: 2321-9653; IC Value: 45.98; SJ Impact Factor: 7.429
Volume 9 Issue IX Sep 2021- Available at www.ijraset.com

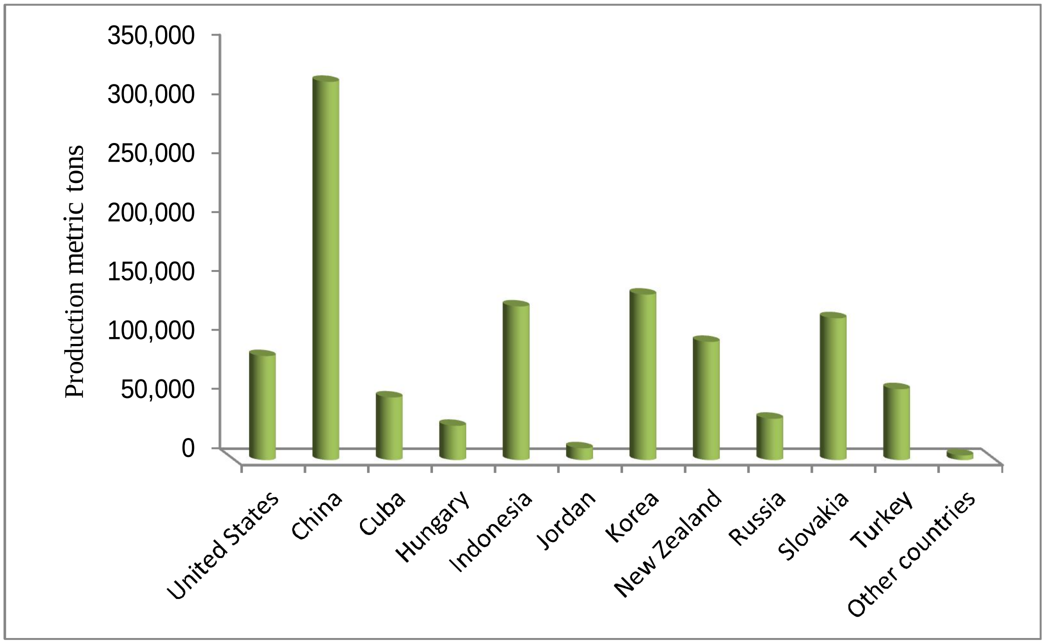


Fig. 1 World production of natural zeolite [54]

The objective of this study is to provide information on geological, geochemical and mineralogical properties of the zeolitic tuffs in Al-Ahyuq area in order to determine their mineralogical constituents and to identify their economic potentials. It also aims to use ASTER data to map the zeolitic tuffs in the study area.

## II. GEOLOGICAL SETTING

The geology of the studied locality shows wide exposures of different types of acidic and basic volcanic rocks including zeolitized tuffs (Fig. 2). Stratigraphic evidence suggests that the sequence of volcanic events from the oldest (at the bottom) to the youngest (at the top). The Yemen volcanic group which belongs to the Tertiary age [55], [56], consists of two subunits of basalt (at bottoms) and rhyolites (at tops). The basaltic flows have a wide thickness with cooling fissures that give them a special characteristic, namely to detach in polyhedron fragments [57]. The basaltic rocks of this area contain small fragments of scoriaceous and are characterized by massive and columnar structures and porphyritic textures. The rhyolitic rocks are compact, vesicular and have columnar structures. They are red, white, and gray in colour and are often associated with ignimbrite. According to [55], the ignimbrites are present at different levels in the sequence and exhibit various degrees of welding, colours and textures. Zeolitic tuffs are associated with rhyolite and volcanic glass. The zeolitic tuffs layers are characterized by white, gray, light- green and yellowish colours and friable composition.

The upper part of the tuffs contain little zeolites. The lithic blocks consist of acidic rocks in close composition to the matrix. The content of zeolites in lower units is rather high compared to the upper units. The degree of lithification of tuffic rocks varies from place to place, where the strongly lithified, tuffic rocks were found as white-yellowish colour and contain a small amount of lithic fragment and high amount of zeolites. Tuffic rocks found as semi-white-gray colour containing a lot of lithic fragments while the degree lithification of tuffic rocks is not strongly lithified. Many types of rocks may contain small amounts of zeolites but the main rock type containing such minerals is the zeolitized volcanic tuff. The volcanoclastic deposits contain large amounts of zeolites, which result from the transformation of volcanic glass and primary aluminosilicate minerals [58]. The main reserves of high quality zeolite deposits in Yemen are located in Taiz, Ibb and Dhamar. According to the Yemen geological survey and mineral resources board the reservoir estimate is 200,000,000 $m^3$[59].

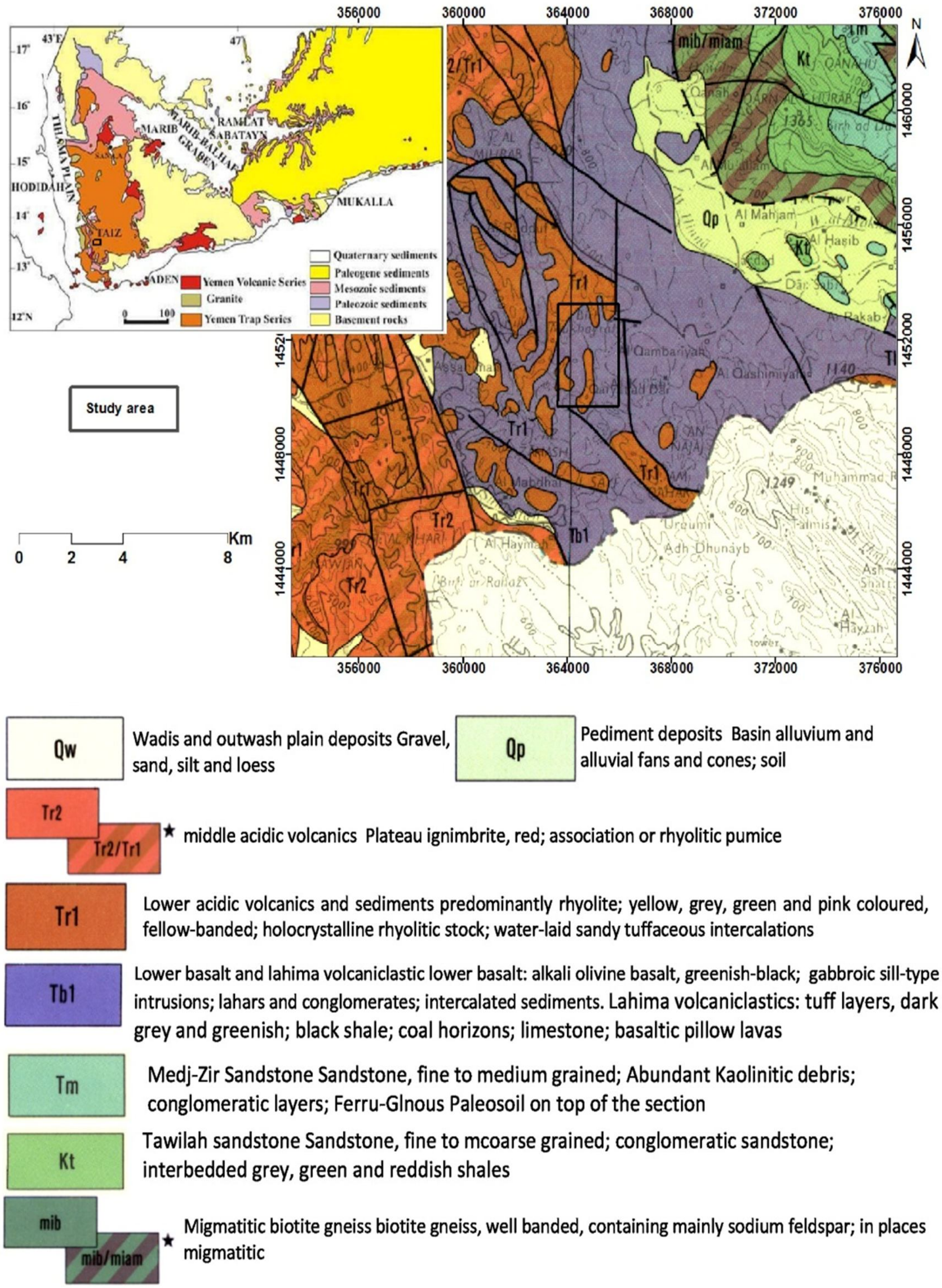


Fig. 2 Geological map of Taiz shows the studied locality of Al-Ahyuq, southwest of Taiz city [60]

## III. METHODOLOGY

The represented samples of Al-Ahyuq zeolitic tuffs were collected, previously described and prepared for various laboratory analysis. X-Ray Diffraction and X-Ray Fluorescence Spectrometer (XRFs) analysis were carried out at the Central Laboratories Sector of Egyptian Mineral Resources Authority (EMRA) and in the Central Laboratories of Geological Survey and Mineral Resources Board (GSMR) Sana'a, Yemen. Samples were prepared for powder XRD by grinding without treatment and testing using XD-2/XD-3 Goniometer Type vertical: 00-2 θ scan: 0-θ scan high, single-phase 508z, 220 v, max. 60kw, rated powder 3kw (GSMR). X-Ray Diffraction method has high degree accuracy and can readily be used to identify individual minerals in mixture of zeolite and non-zeolite minerals [61]. It is the most accurate and commonly used method to identifying zeolite minerals and to provide a semi-quantitative estimate of the percentage present in the sample [27]. Chemical analysis was performed on a portion of selected samples of zeolitic tuffs, analyzing their major oxides using X-Ray Fluorescence Spectrometer (XRFs) techniques, WDXRF 1Kw, S8 Tiger Pruker AXA, AG-RH tube at GSMR, and the other samples were analyzed in EMRA. The pH value was measured at room temperature using a pH meter.

Image processing techniques; colour composite, band ratio, and resamples of spectral reflectance (VNIR and SWIR) were applied to the ASTER data covered Al-Ahyuq area. These techniques were integrated with the Geological, Geochemical and Mineralogical data for studying Al-Ahyuq zeolitic tuffs. Based on the spectral absorption and reflectance characteristics of clinoptilolite mineral and wave length of ASTER bands (Table 1 and Fig. 3), different band ratios were generated: 4/9 and 3/9, and band ratio composite 4/6, 2/1, 3/2.

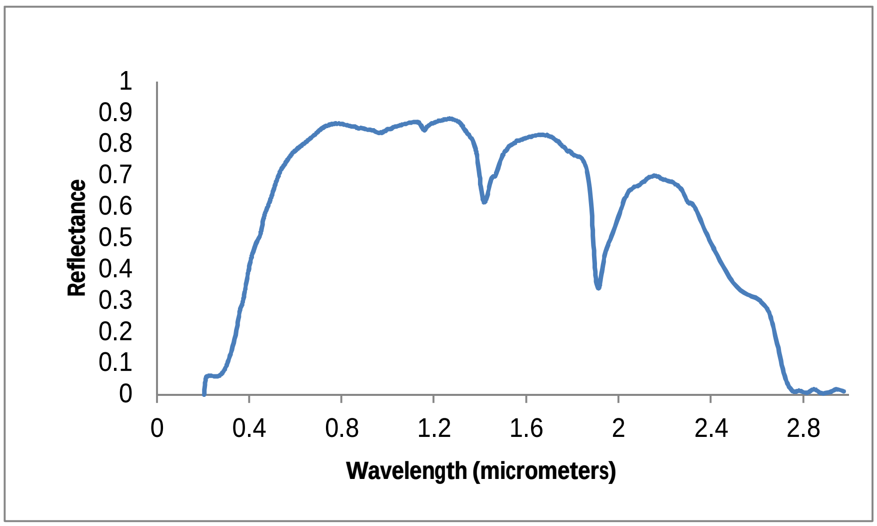


Fig. 3 USGS spectra of clinoptilolite mineral

### A. *Mineralogy of Zeolitic Tuffs*

The mineralogical assemblages of Al-Ahyuq zeolitic tuff samples which were investigated by XRD analyses revealed that they are composed of clinoptilolite as major constituent with high purity. This is inferred from his high peaks intensity in the XRD pattern. The presence of minor peaks related to other zeolites and trace minerals phases of quartz, cristobalite, montmorillonite, calcite and K-feldspars (Fig. 4a, 4b, 4c). It is not possible to reliably distinguished heulandite and Clinoptilolite on the basis of XRD data because of their similarity structural [6], [8], but Si/Al ratio and thermal stability easily differentiate them. The zeolite minerals in Al-Ahyuq area occur as a product hydrothermal alteration of vitric tuffs. The devitrification feature of volcanic glass and zeolite formation represented ubiquitous processes, which indicates that the rocks have been subjected to extensive hydrothermal alteration [63]. Figure 5 shows the SEM images of the surface morphology of the natural clinoptilolite of Al-Ahyuq area which is mentioned in [64], [65].

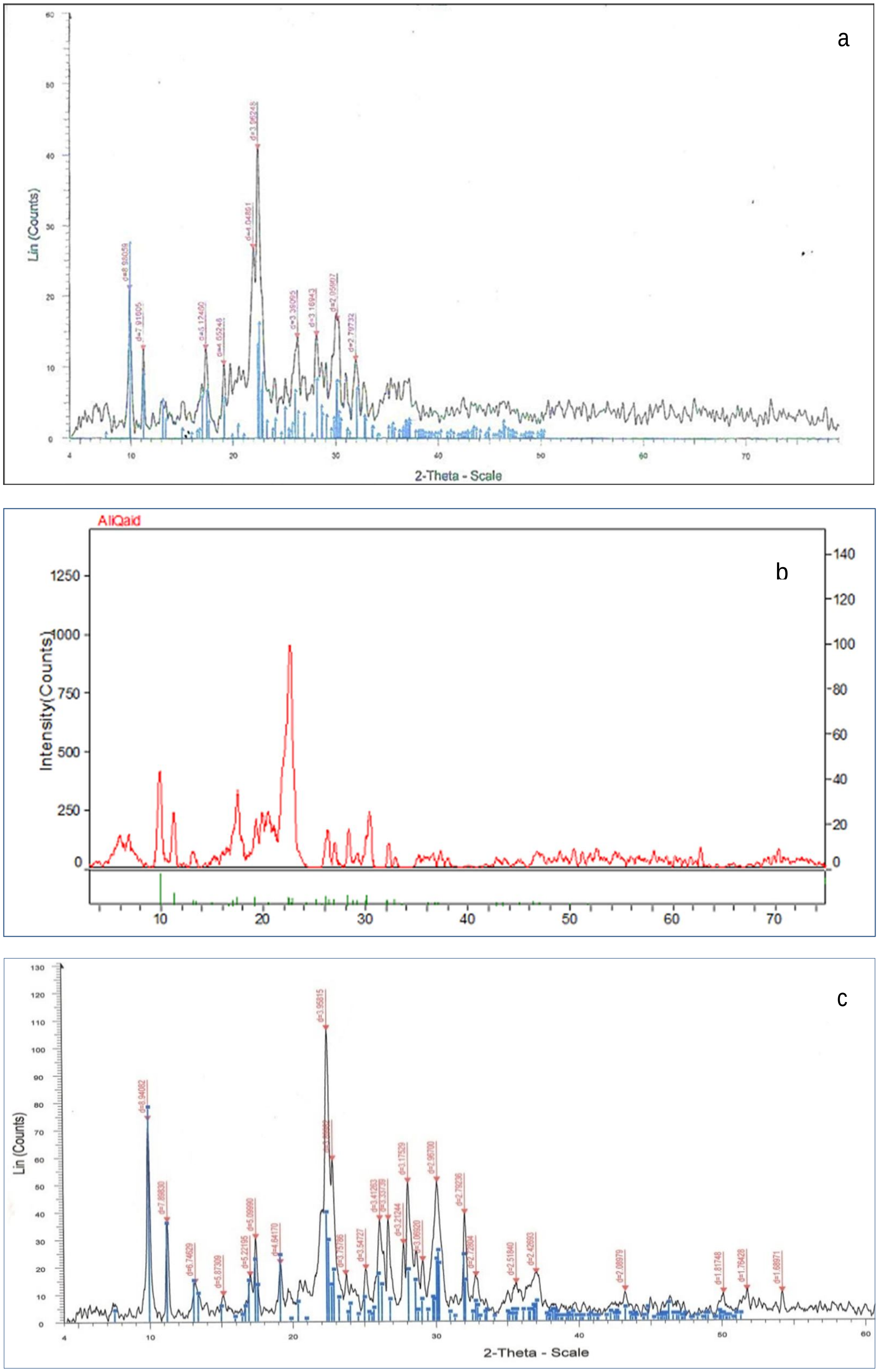


Fig. 4 a, b, c XRD analysis for bulk samples from Al-Ahyuq Zeolitic Tuffs

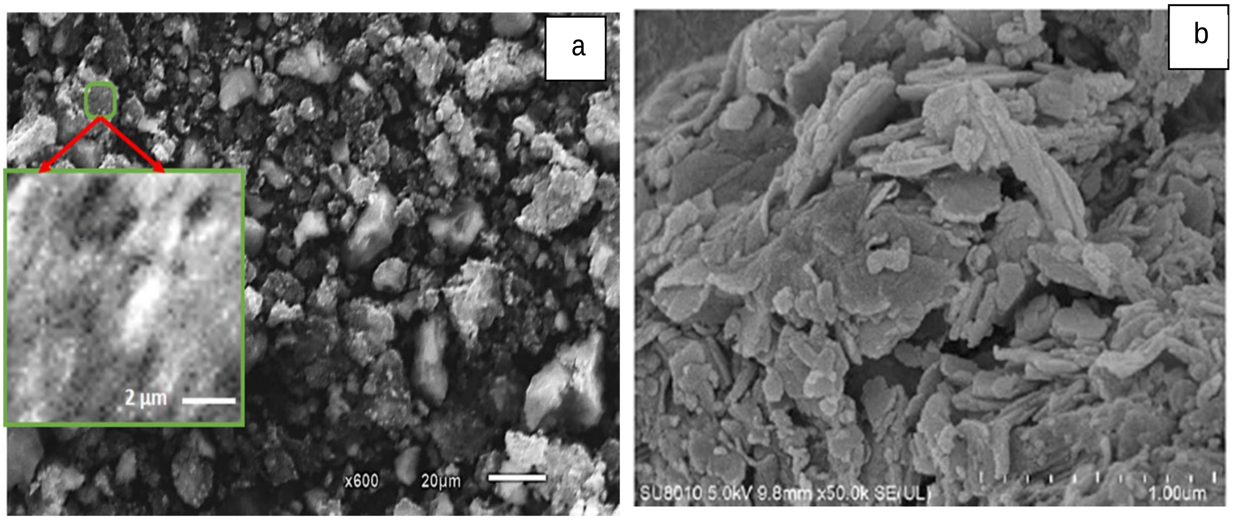


Fig. 5 SEM images of the surface morphology of the natural clinoptilolite of Al-Ahyuqe area, a. [64] and b. [65]

*B. Geochemistry*

The chemical analysis results of ten selected samples representing Al-Ahyuq zeolitic tuffs indicated that the concentration of silica oxide is ranging from 63.10 to 71.1 wt% and $Al_2O_3$ from 10.83 to 12.07 wt%. $K_2O$ ranges from 2.50 to 5.16 wt%, $Na_2O$ from 0.12 to 1.89 wt% and $Fe_2O_3$ from 2.06 to 2.65 wt%, whereas CaO ranges from 1.01 to 2.58 wt%, the remaining oxides are present only in a small concentration (Table 2).

The $Al_2O_3$wt.%, total alkalis ($Na_2O+K_2O$ wt.%), and CaO versus $SiO_2$ wt.% display proportional relationships indicating that they exhibit similar geochemical behavior under the zeolitization process (Fig. 6a, 6b, 6c and Table 3). They show a steady decrease with increasing of $SiO_2$ (strong negative correlation). MnO, $K_2O$ and $P_2O_5$ also show slightly tend to decrease with increasing $SiO_2$ (Fig. 6d and Table 3). Potassium has Clearly been affected by redistribution processes, exhibiting in some samples gains relatively to a presumed initial magmatic content.

The value of LOI ranging from 8.4 to 12.8 wt%. CaO, $Al_2O_3$ and $Na_2O$ exhibits strong positive correlation with LOI however $K_2O$ and $Fe_2O_3$ reveal negative correlation (Table 3). $SiO_2$ shows strong negative correlation with LOI (Fig. 6e and Table 3). This indicates that the samples are highly altered and display several stages of alteration.

The presence of CaO in selected samples indicates presence of carbonates and presence of minor amounts of $SO_3$ may indicate the occurrence of traces of gypsum. Zeolitic tuffs combine mainly of altered volcanic glass, their original chemical composition should reflect the chemistry of the volcanic rocks from which they were derived [61]. The pH measurement is the measure of the acidity or alkalinity of a solution which is around of pH 8. Due to all samples having Si/Al value greater than 4 with an average 5.2 wt%, the presence of clinoptilolite is clearly demonstrated.

It is directly proportional to the thermal stability. The above results enhanced the suitability of using Al-Ahyuq zeolites in water purification, as an additive to animal foods, in agriculture and as an adsorbent for the removal of heavy metals from the wastewater. Recently, local Companies such as Green Space Ltd and SROR started to trade Al-Ahyuq zeolite as a food for animals and for agricultural applications as slow release fertilizers, increasing the nutrient, water use efficiency, treating salinity, and increasing crop yield. Al-Ahyuq zeolitic tuff was found to be highly effective at removing iron from ground water. The results of chemical analyses indicate that the zeolitized volcanic tuffs from Al-Ahyuq were derived from a rock of acidic composition. Zeolites are the most common products of transformation of silicic volcanic glass in Al-Ahyuq area.

Table 2: Chemical Composition Of Selected Samples Of Al-Ahyuq Zeolitic Tuffs (Major Oxides WT%)

| Major Oxides% | ZAH-1 | ZAH-2 | ZAH-3 | ZAH-4 | ZAH-5 | ZAH-6 | ZAH-7 | ZAH-8 | ZAH-9 | ZAH-10 | Average |
|---|---|---|---|---|---|---|---|---|---|---|---|
| $SiO_2$ | 69.68 | 70.06 | 70.5 | 67.30 | 63.10 | 67.01 | 70.6 | 71.10 | 69.9 | 67.60 | 68.69 |
| $Al_2O_3$ | 12.07 | 11.2 | 11.72 | 11.58 | 13.70 | 11.3 | 10.83 | 11.5 | 11.8 | 11.59 | 11.73 |
| $Fe_2O_3$ | 2.18 | 2.06 | 2.56 | 2.21 | 2.32 | 2.40 | 2.65 | 2.35 | 2.5 | 2.55 | 2.38 |
| CaO | 1.16 | 1.62 | 1.01 | 2.23 | 1.89 | 2.58 | 1.68 | 1.50 | 1.28 | 1.89 | 1.68 |
| MgO | 0.52 | 0.34 | 0.48 | 0.47 | 0.10 | 0.87 | 0.33 | 0.33 | 0.46 | 0.52 | 0.44 |
| $Na_2O$ | 0.4 | 0.12 | 0.35 | 0.42 | 1.89 | 0.32 | 0.30 | 0.16 | 0.43 | 0.26 | 0.47 |
| $K_2O$ | 3.03 | 5.16 | 4.57 | 3.92 | 4.13 | 2.5 | 2.51 | 3.59 | 3.17 | 4.28 | 3.69 |
| MnO | 0.16 | 0.08 | 0.09 | 0.9 | 0.04 | 0.14 | 0.08 | 0.08 | 0.1 | 0.06 | 0.17 |
| $P_2O_5$ | 0.03 | 0.01 | 0.02 | 0.36 | 0.02 | 0.01 | 0.01 | 0.01 | 0.02 | 0.03 | 0.05 |
| $TiO_2$ | 0.16 | 0.15 | 0.16 | 0.24 | LDL | 0.13 | 0.21 | 0.21 | 0.16 | 0.23 | 0.17 |
| $SO_3$ | 0.002 | 0.002 | 0.007 | 0.006 | 0.004 | 0.002 | 0.007 | 0.005 | 0.003 | 0.001 | 0.00 |
| LOI | 10.55 | 9.08 | 8.4 | 10.32 | 12.8 | 12.5 | 9.50 | 9.12 | 10.1 | 9.84 | 10.22 |
| Total | 99.94 | 99.88 | 99.87 | 99.96 | 99.99 | 99.76 | 99.71 | 99.95 | 99.92 | 98.85 | 99.68 |
| Si/Al | 5.10 | 5.52 | 5.31 | 5.13 | 4.07 | 5.24 | 5.76 | 5.46 | 5.23 | 5.15 | 5.20 |

Table 3: Correlation Matrix Of Pearson Of Major Oxides Of Al-Ahyuq Zeolitic Tuff Samples

| Oxides | $SiO_2$ | $Al_2O_3$ | $Fe_2O_3$ | CaO | MgO | $Na_2O$ | $K_2O$ | MnO | $P_2O_5$ | $TiO_2$ | $SO_3$ | LOI |
|---|---|---|---|---|---|---|---|---|---|---|---|---|
| $SiO_2$ | 1.00 | | | | | | | | | | | |
| $Al_2O_3$ | -0.73 | 1.00 | | | | | | | | | | |
| $Fe_2O_3$ | 0.15 | -0.19 | 1.00 | | | | | | | | | |
| CaO | -0.60 | -0.06 | -0.11 | 1.00 | | | | | | | | |
| MgO | 0.14 | -0.48 | 0.11 | 0.35 | 1.00 | | | | | | | |
| $Na_2O$ | -0.82 | 0.92 | -0.06 | 0.14 | -0.54 | 1.00 | | | | | | |
| $K_2O$ | -0.08 | 0.21 | -0.36 | -0.22 | -0.41 | 0.08 | 1.00 | | | | | |
| MnO | -0.15 | -0.11 | -0.34 | 0.38 | 0.15 | -0.09 | 0.02 | 1.00 | | | | |
| $P_2O_5$ | -0.21 | -0.04 | -0.31 | 0.37 | 0.05 | -0.02 | 0.10 | 0.99 | 1.00 | | | |
| $TiO_2$ | 0.63 | -0.78 | 0.19 | -0.03 | 0.32 | -0.83 | -0.10 | 0.40 | 0.38 | 1.00 | | |
| $SO_3$ | 0.23 | -0.11 | 0.35 | -0.20 | -0.34 | 0.05 | -0.06 | 0.29 | 0.30 | 0.17 | 1.00 | |
| LOI | -0.84 | 0.58 | -0.16 | 0.63 | 0.13 | 0.68 | -0.37 | 0.04 | 0.03 | -0.65 | -0.35 | 1.00 |

ISSN: 2321-9653; IC Value: 45.98; SJ Impact Factor: 7.429
Volume 9 Issue IX Sep 2021- Available at www.ijraset.com

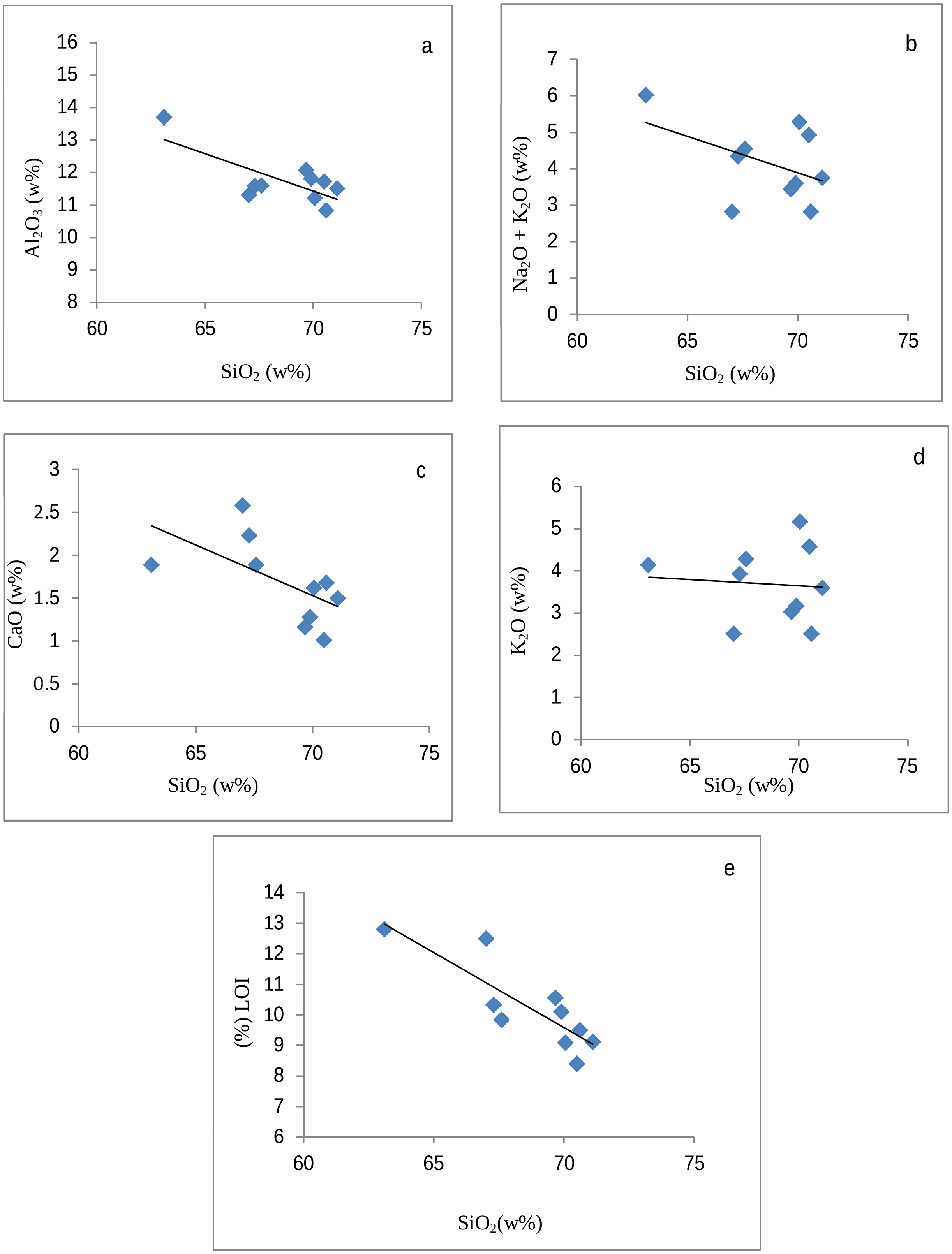


Fig. 6 Diagrams of selected major oxides of Al-Ahyuq Zeolitic Tuffs (a) $SiO_2$% vs. $Al_2O_{3\%}$, (b) $SiO_2$% vs. $K_2O$ (c) (d) $SiO_{2\%}$ vs. $(Na_2O+K_2O)$% (f) $SiO_{2\%}$ vs. (CaO)% and (f) $SiO_{2\%}$ vs. LOI%.

## V. COMPARISON OF THE STUDIED ZEOLITIC TUFF OF AL-AHYUQ WITH THE WORLD ZEOLITE ANALYSES

The Comparison of the average of chemical analyses of Al-Ahyuq zeolitic tuffs with zeolite deposits) from Italy, Australia, Romania, Greece, Serbia and Turkey gives a good idea about the chemical composition of the zeolite deposits and its validity for industrial, medical and agricultural uses (Table 4). Figure 7 shows the relationships of major oxides of Al-Ahyuq zeolite deposits compared to other world's deposits. Generally, it is clear that the Al-Ahyuq zeolite deposit has a higher $K_2O$, and lower $Na_2O$ and CaO content compared to these found in other world's deposit. The results of chemical analyses of Al-Ahyuq zeolitic tuff samples are within the range of the chemical analyses of the world's similar deposits.

Table 4: The Average Chemical Analyses Of AL-AHYUQ Zeolitic Tuffs Compared With Other Chemical Analyses From Different Countries 1[61] 2 [66] 3[67] 4[68] 5[63] 6[28]

| Oxides (%) | Al-Ahyuq Yemen | [1]Romania | [2]Turkey | [3]Australia | [4]Greece | [5]Italy | [6]Serbia |
|---|---|---|---|---|---|---|---|
| $SiO_2$ | 68.69 | 63.98 | 71.3 | 68.26 | 69.71 | 67.25 | 68.5 |
| $Al_2O_3$ | 11.73 | 14.53 | 11.5 | 12.99 | 11.84 | 11.99 | 12.77 |
| $Fe_2O_3$ | 2.38 | 1.71 | 0.54 | 1.37 | 4.53 | 2.00 | 2.78 |
| MgO | 0.44 | 0.23 | 0.93 | 0.83 | 0.53 | 1.04 | 1.11 |
| CaO | 1.68 | 5.46 | 2.98 | 2.09 | 5.15 | 2.08 | 3.22 |
| $Na_2O$ | 0.47 | 1.00 | 0.39 | 0.64 | 1.09 | 1.23 | 0.78 |
| $K_2O$ | 3.69 | 0.88 | 3.15 | 4.11 | 0.9 | 3.00 | 1.12 |
| LOI | 10.22 | 11.86 | 9.09 | 8.87 | 13.23 | 10.99 | 9.55 |

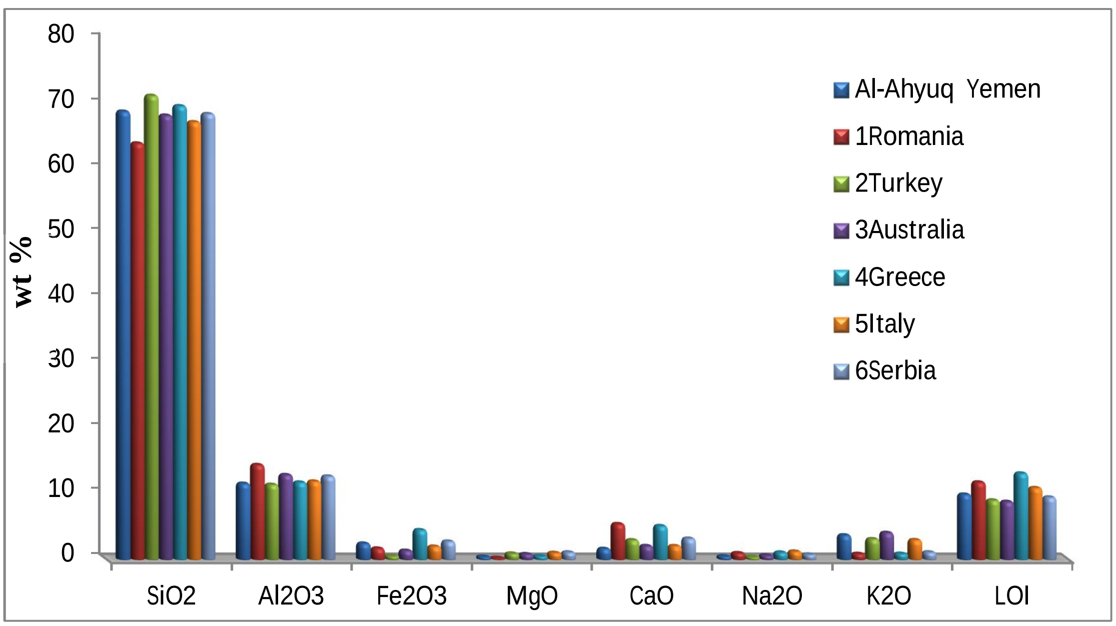


Fig. 7 Percentage (Wt%) of $SiO_2$, $Al_2O_3$, LOI, $Fe_2O_3$, MgO, $Na_2O$, $K_2O$ and CaO of Al-Ahyuq zeolitic tuffs compared with the other countries

### *A. ASTER Data Interpretation*

The false colour composite of ASTER bands (4R,3G,2 B) enhanced the zeolitic tuff and showed it as bright pixels due to the high reflected energy of zeolite in these bands (Fig. 8). The band ratio 3/9 is found to be a favorable ratio for mapping Al-Ahyuq zeolitic tuffs. The zeolites highlighted as bright pixel because they have a high reflectance on band 3 and low reflectance in band 9 of ASTER image (Fig. 3, 9). Vegetation cover on this ratio also enhanced with bright pixel. The band ratio 4/6 is a good hydrothermal alteration indicator, which highlighted zeolitic tuffs in bright pixels, as OH-bearing zeolites exhibits high reflectance in band 4 and low reflectance in band 6. It emphasizes the contrast between the zeolite deposit, and sandstone (bright pixels) and surrounding rock unites (dark pixels) (Fig. 10).

Band ratio image (4/6-R, 2/1-G and 3/2-B) shows that the zeolitic tuffs are well separated from the adjacent rocks and illustrated as orange colour (Fig. 11). Spectra after being resampled to ASTER VNIR+SWIR bands of the study area comparing with the USGS library spectra of zeolite – clinoptilolite as reference shows that the zeolite deposit of Al-Ahyuq is almost identically with the reference clinoptilolite (Fig. 12).

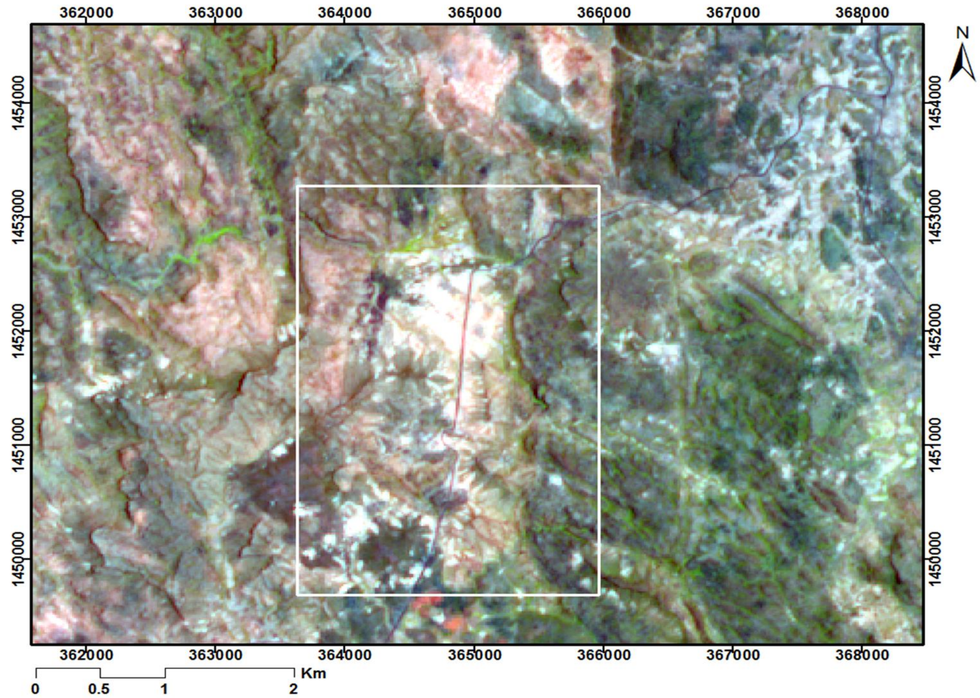


Fig.8 The colour composite of ASTER image (R:4, G:3, B:2) shows zeolite deposits as white colour

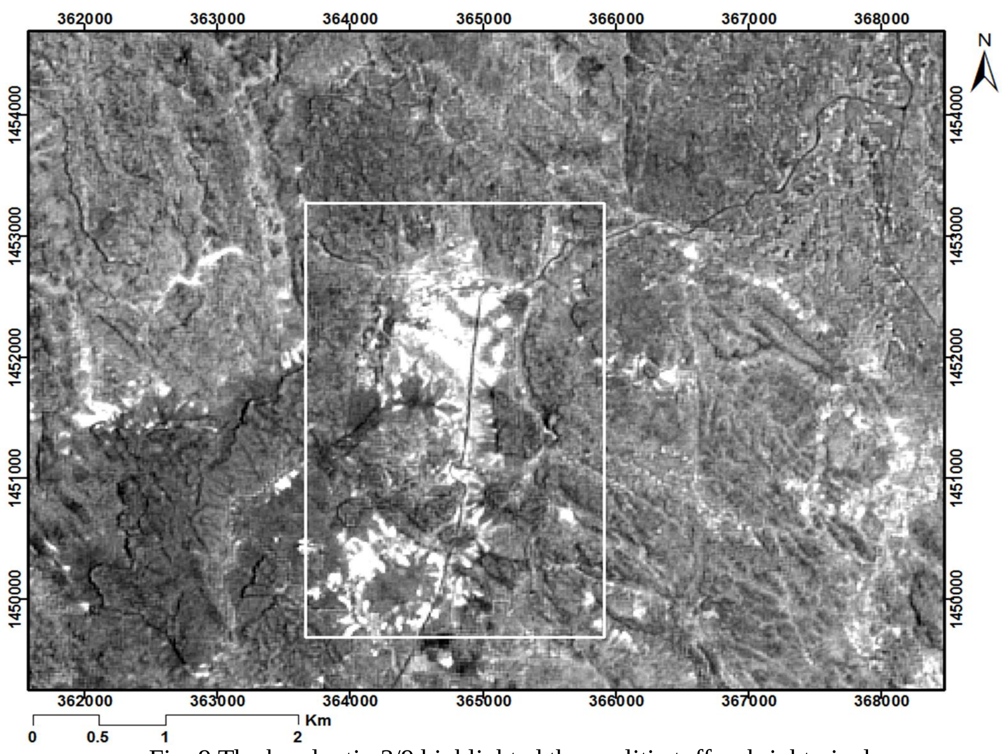


Fig. 9 The band ratio 3/9 highlighted the zeolitic tuff as bright pixel

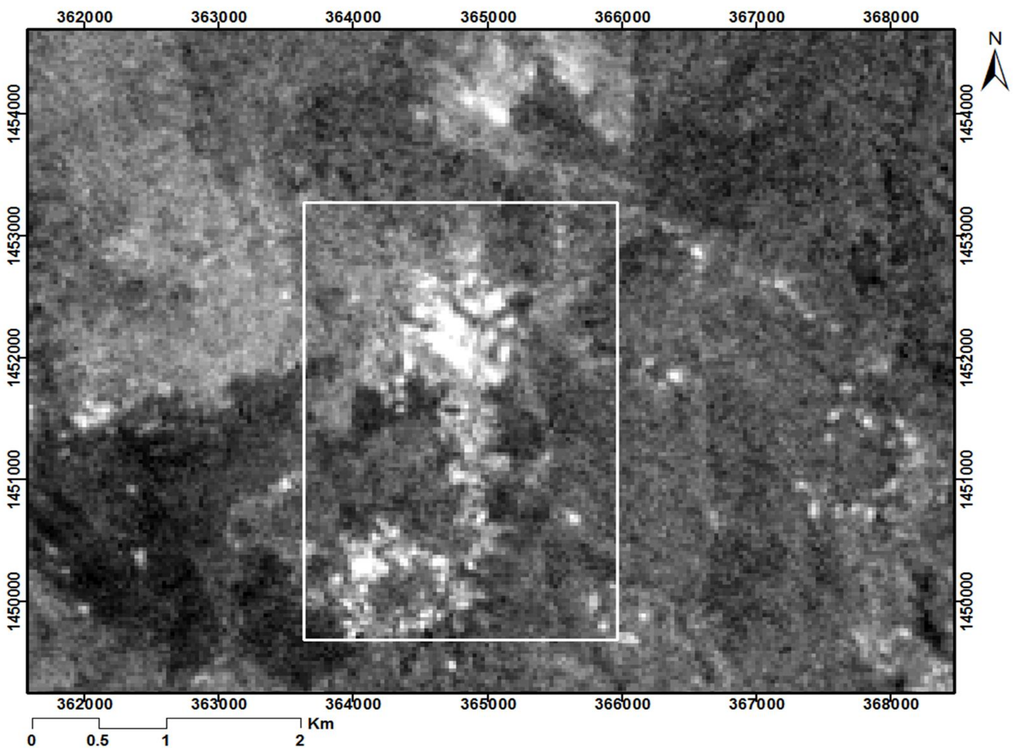


Fig.10 band ratio 4/6 highlighted the ore deposits of zeolite as bright pixels

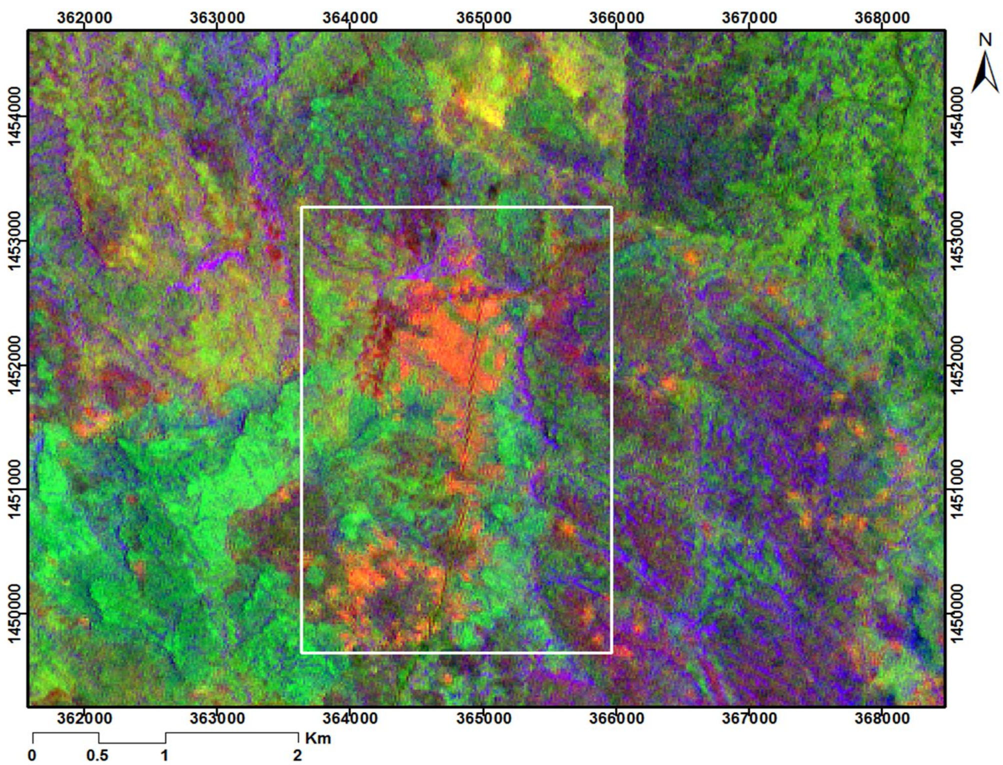


Fig. 11 Band ratio image (4/6-R, 2/1-G and 3/2-B) enhanced zeolite deposits as orange

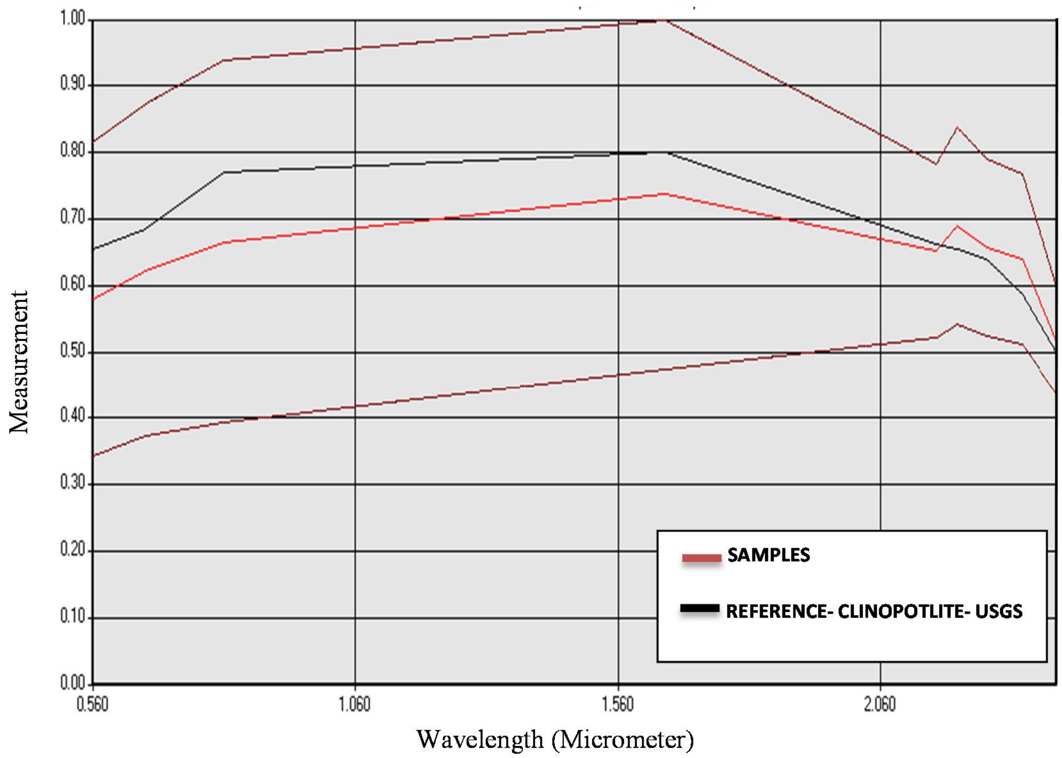


Fig. 12 Spectra after being resampled to ASTER VNIR+SWIR bands and USGS library spectra Clinopotlite - references

## VI. CONCLUSIONS

Mineralogical studies showed that the zeolite minerals of Al-Ahyuq area are composed of clinoptilolite as major constituent with traces of other zeolite minerals. XRF analysis results showed that the concentration of $SiO_2$ with an average 68.69 wt%, $Al_2O_3$ 11.73 wt%, $Fe_2O_3$ 2.38 wt%, CaO 1.68 wt% and $K_2O$ 3.69 wt%.

The other oxides are present in a small concentration. The value of LOI ranging from 8.4 wt% to 12.8 wt% with an average 10.22 wt% and exhibits strong negative correlation with $SiO_2$. The Si/Al ratio with an average 5.2 wt% that enhanced the that the clinoptilolite is the main constituent mineral of Al-Ahyuq zeolitic tuff. The comparison result of chemical analyses of Al-Ahyuq zeolites with world zeolite revealed that Al-Ahyuq zeolite within the range of the chemical analyses of the world's similar zeolite deposits.

The zeolitized volcanic tuffs from Al-Ahyuq are mainly represented by acid vitric tuffs. Zeolites formed as a result of the reaction between hydrothermal and rock components volcanics such as tuffs, rhyolites and volcanic glass. Based on ASTER data processing; band ratios, colour composition and resampling spectral library to VNIR and SWIR ASTER bands, it is concluded that the study area is affected by hydrothermal alteration processes resulting in widespread of zeolite deposits. These processes were also successfully used to mapping zeolite deposits. Due to of the unique mineralogical, physical and chemical properties of zeolites, they are very useful in a variety of applications in agronomy, ecology, certain manufacturing, industrial processes, medicine, and cosmetics.

## VII. ACKNOWLEDGEMENTS

The authors are grateful to Green Space Ltd, and SROR zeolite company for great help. Also, they would like to thank Ms. DI Kristina Stocker, Dr. Badeea Asweedy, Dr. Angela Mormone and Dr. Khadijeh Validabadi for the valuable comments that helped in improving the manuscript.

## REFERENCES

[1] M. Onal, T. Depci, C. Ceylan, and N. Kizilkaya, "The Zeolite Deposit of Hekimhan in the Malatya Basin," in World Multidisciplinary Earth Sciences Symposium (WMESS 2016), IOP Conference Series: Earth and Environmental Science, 2016, vol. 44, no. 4, p. 42011.

[2] M. Almjadleh, S. Alasheh, and I. Raheb, "Use of natural and modified Jordanian zeolitic tuff for removal of cadmium(II) from aqueous solutions," Jordan J. Civ. Eng., vol. 8, no. 3, pp. 332–343, 2014.

[3] G. Kirov and L. Filizova, "Cationic hydration impact on zeolite formation and properties: A review and discussion," Geochem. Miner. Pet. Sofia, vol. 49, pp. 65–82, 2012.

[4] S. Ivkovic, U. Deutsch, A. Silberbach, E. Walraph, and M. Mannel, "Dietary supplementation with the tribomechanically activated zeolite clinoptilolite in immunodeficiency: effects on the immune system," Adv. Ther., vol. 21, no. 2, pp. 135–147, 2004.

[5] F. A. Mumpton and P. H. Fishman, "The application of natural zeolites in animal science and aquaculture," J. Anim. Sci., vol. 45, no. 5, pp. 1188–1203, 1977.

[6] D. L. Bish and J. W. Carey, "Thermal behavior of natural zeolites," Rev. Mineral. Geochemistry, vol. 45, no. 1, pp. 403–452, 2001.

[7] D. S. Papaioannou, C. S. Kyriakis, C. Alexopoulos, E. D. Tzika, Z. S. Polizopoulou, and S. C. Kyriakis, "A field study on the effect of the dietary use of a clinoptilolite-rich tuff, alone or in combination with certain antimicrobials, on the health status and performance of weaned, growing and finishing pigs," Res. Vet. Sci., vol. 76, no. 1, pp. 19–29, 2004.

[8] K. Stocker, M. Ellersdorfer, M. Lehner, and J. G. Raith, "Characterization and utilization of natural zeolites in technical applications," BHM Berg-und Hüttenmännische Monatshefte, vol. 162, no. 4, pp. 142–147, 2017.

[9] F. Shariatmadari, "The application of zeolite in poultry production," Worlds. Poult. Sci. J., vol. 64, no. 1, pp. 76–84, 2008.

[10] E. Ozturk, G. Erener, and M. Sarica, "Influence of natural zeolite on performance of laying hens and egg quality," Turkish J. Agric. For., vol. 22, no. 6, pp. 623–628, 1998.

[11] P. P. Diale, E. Muzenda, and J. Zimba, "A study of South African natural zeolites properties and applications," in Proceedings of the World Congress on Engineering and Computer Science, 2(WCECS), 2011, vol. 2, pp. 19–21.

[12] A. M. Al-Hawbani and A. F. Maky, "Petrography and Mineralogy of Zeolite Deposits, Mareya Area Southwest Thamar, Yemen," Curr. Sci. Int., vol. 7, no. 2, pp. 204–212, 2018.

[13] S. KraljeviC PaveliC, J. Simovic Medica, D. Gumbarevic, A. Filosevic, N. Przulj, and P. Kresimir, "Critical review on zeolite clinoptilolite safety and medical applications in vivo," Front. Pharmacol., vol. 9, p. 1350, 2018.

[14] F. A. Mumpton, "La roca magica: Uses of natural zeolites in agriculture and industry," Proc. Natl. Acad. Sci., vol. 96, no. 7, pp. 3463–3470, 1999.

[15] V. J. Inglezakis and A. A. Zorpas, Handbook of natural zeolites. Bentham Science Publishers Ltd., 2012.

[16] S. Wang and Y. Peng, "Natural zeolites as effective adsorbents in water and wastewater treatment," Chem. Eng. J., vol. 156, no. 1, pp. 11–24, 2010.

[17] C.H. Yu, C.H. Huang, C.S. Tan, and others, "A review of CO2 capture by absorption and adsorption," Aerosol Air Qual. Res., vol. 12, no. 5, pp. 745–769, 2012.

[18] K. Margeta, N. Z. Logar, M. Siljeg, and A. Farkas, "Natural zeolites in water treatment-how effective is their use," in Water treatment, vol. 5, InTech, London, UK, 2013, pp. 81–112.

[19] B. Faccini et al., "Ammonium-exchanged zeolitite preparation for agricultural uses: From laboratory tests to large-scale application in Zeolite project prototype," Period. di Mineral., vol. 84, no. 2, pp. 303–321, 2015, doi: 10.2451/2015PM0015.

[20] P. Palanivell, O. H. Ahmed, and N. M. Ab Majid, "Minimizing ammonia volatilization from urea, improving lowland rice (cv. MR219) seed germination, plant growth variables, nutrient uptake, and nutrient recovery using clinoptilolite zeolite," Arch. Agron. Soil Sci., vol. 62, no. 5, pp. 708–724, 2016.

[21] M. Sprynskyy, B. Buszewski, A. P. Terzyk, and J. Namieśnik, "Study of the selection mechanism of heavy metal ($Pb^{2+}$, $Cu^{2+}$, Ni2+, and $Cd^{2+}$) adsorption on clinoptilolite," J. Colloid Interface Sci., vol. 304, no. 1, pp. 21–28, 2006.

[22] Y. Orhan and S. Kocaoba, "Adsorption of toxic metals by natural and modified clinoptilolite," Ann. di Chim. J. Anal. Environ. Cult. Herit. Chem., vol. 97, no. 8, pp. 781–790, 2007.

[23] Y. F. Tao, Y. Qiu, S. Y. Fang, Z. Y. Liu, Y. Wang, and J. H. Zhu, "Trapping the lead ion in multi-components aqueous solution by natural clinoptilolite," J. Hazard. Mater., vol. 180, no. 1–3, pp. 282–288, 2010.

[24] M. Beltcheva et al., "Zeolites versus lead toxicity," J. Bioequiv. Availab, vol. 7, pp. 12–29, 2015.

[25] E. Polat, M. Karaca, H. Demir, and A. N. Onus, "Use of natural zeolite (clinoptilolite) in agriculture," J. fruit Ornam. plant Res., vol. 12, no. 1, pp. 183–189, 2004.

[26] R. Al Dwairi, "Characterization of Pozzolana from Tafila area and its potential use as soil amendment for plant growth," Jordan J. Earth Environ. Sci., vol. 6, no. 3, pp. 35–40, 2014.

[27] K. M. Ibrahim, "Geology and mineralogy of Zeolitic Tuff in Tulul Unuqar Rustum Ash Shmaliyya, NE Jordan," Jordan J Earth Env. Sci, vol. 6, no. 3, pp. 29–34, 2014.

[28] M. R. Tomasevic-Canovic, "Purification of natural zeolite-clinoptilolite for medical application: Extraction of lead," J. Serbian Chem. Soc., vol. 70, no. 11, pp. 1335–1345, 2005.

[29] H. Khan, A. . Z. Khan, R. Khan, and T. Henmi, "Influence of zeolite application on germination and seed quality of soybean down on allophanic soil," Res. J. seed Sci., vol. 2, no. 1, pp. 1–8, 2009.

[30] M. Zhang, B. Gao, J. Chen, and Y. Li, "Effects of graphene on seed germination and seedling growth," J. Nanoparticle Res., vol. 17, no. 2, pp. 1–8, 2015.

[31] D. Di Giuseppe, J. Ibanez, M. Melchiorre, and M. Coltorti, "On the potential effect of micronized zeolites on seed germination: a prospective study," Period. di Mineral., vol. 87, no. 1, 2018.

[32] I. M. Dwairi, "Conserving toxic ammoniacal nitrogen in manure using natural zeolite tuff: a comparative study," Bull. Environ. Contam. Toxicol., vol. 60, no. 1, pp. 126–133, 1998.

[33] X. Karamanlis et al., "The effect of a natural zeolite (clinoptilolite) on the performance of broiler chickens and the quality of their litter," Asian-Australasian J. Anim. Sci., vol. 21, no. 11, pp. 1642–1650, 2008.

[34] M. Safaeikatouli, F. Boldaji, B. Dastar, and S. Hassani, "The effect of dietary silicate minerals supplementation on apparent ileal digestibility of energy and protein in broiler chickens," Int. J. Agric. Biol., vol. 14, no. 2, 2012.

[35] T. Andronikashvili, K. Pagava, T. Kurashvili, and L. Eprikashvili, "Possibility of Application of Natural Zeolites for Medicinal Purposes," Bull. Georg. Natl. Acad. Sci., vol. 3, no. 2, pp. 158–167, 2009.

[36] A. Mormone, M. R. Ghiara, G. Balassone, M. Piochi, R. Lonis, and M. Rossi, "High-silica zeolites in pyroclastic flows from Central Sardinia (Italy): clues on genetic processes and reserves from a mineralogical study," Mineral. Petrol., vol. 112, no. 6, pp. 767–788, 2018.

[37] M. V. Cattaneo and T. M. Chang, "The potential of a microencapsulated urease-zeolite oral sorbent for the removal of urea in uremia.," ASAIO Trans., vol. 37, no. 2, pp. 80–87, 1991.

[38] N. Zarkovic et al., "Anticancer and antioxidative effects of micronized zeolite clinoptilolite.," Anticancer Res., vol. 23, no. 2B, pp. 1589–1595, 2003.

[39] J.-H. Shen, Y.-S. Wang, J.-P. Lin, S.-H. Wu, and J.-J. Horng, "Improving the indoor air quality of respiratory type of medical facility by zeolite filtering," J. Air \& Waste Manag. Assoc., vol. 64, no. 1, pp. 13–18, 2014.

[40] L. C. Rowan, S. J. Hook, M. J. Abrams, and J. C. Mars, "Mapping hydrothermally altered rocks at Cuprite, Nevada, using the Advanced Spaceborne Thermal Emission and Reflection Radiometer (ASTER), a new satellite-imaging system," Econ. Geol., vol. 98, no. 5, pp. 1019–1027, 2003.

[41] M. H. Tangestani, N. Mazhari, B. Agar, and F. Moore, "Evaluating Advanced Spaceborne Thermal Emission and Reflection Radiometer (ASTER) data for alteration zone enhancement in a semi-arid area, northern Shahr-e-Babak, SE Iran," Int. J. Remote Sens., vol. 29, no. 10, pp. 2833–2850, 2008.

[42] S. Rajendran, A. Thirunavukkarasu, G. Balamurugan, and K. Shankar, "Discrimination of iron ore deposits of granulite terrain of Southern Peninsular India using ASTER data," J. Asian Earth Sci., vol. 41, no. 1, pp. 99–106, 2011.

[43] A. Rezaei, H. Hassani, P. Moarefvand, and A. Golmohammadi, "Lithological mapping in Sangan region in Northeast Iran using ASTER satellite data and image processing methods," Geol. Ecol. Landscapes, vol. 4, no. 1, pp. 59–70, 2020.

[44] K. V. Bozcheloei and M. H. Tangestani, "Prospecting for Clinoptilolite-Type Zeolite in a Volcano-Sedimentary Terrain Using ASTER Data: A Case Study from Alborz Mountains, Northern Iran," Nat. Resour. Res., vol. 28, 2019, doi: 10.1007/s11053-019-09452-1.

[45] F. F. Sabins, Remote sensing : principles and interpretation /, 3rd ed. New York: W.H. Freeman and Co., 1997.

[46] F. F. Sabins, "Remote sensing for mineral exploration," Ore Geol. Rev., vol. 14, no. 3–4, pp. 157–183, 1999, [Online]. Available: http://dx.doi.org/10.1016/S0169-1368(99)00007-4.

[47] S. A. Drury, Image Interpretation in Geology, 3rd ed. Malden, Mass., Blackwell Science, 2001.

[48] J. R. Jensen, Introductory digital image processing : a remote sensing perspective /, 3rd ed. Upper Saddle River, N.J. : Prentice Hall, 2005

[49] S. Al-Rawashdeh, B. Saleh, and M. Hamzah, "The use of remote sensing technology in geological investigation and mineral detection in El Azraq-Jordan," Cybergeo Eur. J. Geogr., pp. 1–22, 2006.

[50] A. K. Thurmond, M. G. Abdelsalam, and J. B. Thurmond, "Optical-radar-DEM remote sensing data integration for geological mapping in the Afar Depression, Ethiopia," J. African Earth Sci., vol. 44, no. 2, pp. 119–134, 2006.

[51] M. F. Iqbal, M. R. Khan, and A. H. Malik, "Land use change detection in the limestone exploitation area of Margalla Hills National Park (MHNP), Islamabad, Pakistan using geo-spatial techniques," J. Himal. Earth Sci., vol. 46, no. 1, pp. 89–98, 2013.

[52] H. T. Basavarajappa, L. Jeevan, S. Rajendran, and M. C. Manjunatha, "Discrimination of Banded Magnetite Quartzite (BMQ) Deposits and Associated Lithology of Parts of Chikkanayakanahalli Schist Belt of Dharwar Craton, Karnataka, India using Remote Sensing Technique," Int. J. Adv. Remote Sens. GIS, vol. 4, no. 1, pp. 1033–1044, 2015.

[53] T. M. Lillesand and R. W. Kiefer, Remote sensing and image interpretation, 4th ed. New York: John Wiley & Sons, Inc., 2000.

[54] U.S. Geological Survey, "Mineral commodity summaries 2021," 2021. [Online]. Available: https://doi.org/10.3133/mcs2021.

[55] M. Al-Kadasi, "Temporal and spatial evaluation of the basal flow of the Yemen volcanic group," Royal Holloway, University of London, 1994.

[56] Z. R. Beydoun et al., "International lexicon of stratigraphy V. III, Republic of Yemen," in IInternational union of geological sciences and ministry of oil and mineral resources, 2nd ed., 1988, p. 245.

[57] A. M. Al Sabri, "Geology, Mineralogy and origin of zeolite deposits Al Adnah area east Taiz, Yemen," Sana'a University, 2003.

[58] R. L. Hay and R. A. Sheppard, "Occurrence of zeolites in sedimentary rocks: An overview," Rev. Mineral. geochemistry, vol. 45, no. 1, pp. 217–234, 2001.

[59] NMSS, "National Mining Sector Strategy-2020-2030, Sana'a," 2020.

[60] W. Kruck and Schaffer, U., "Geological Map of the Republic of Yemen Sheet Ta'izz, Ministry of Oil and Mineral Resources, Sana'a, Yemen," Fed. Inst. Geosci. Nat. Resour. Hann., 1991.

[61] H. Bedelean, V. Codrea, and O. Barbu, "Geological and mineralogical characterization of some zeolitized tuffs from NWrn Transylvania, Romania," Bull. Geol. Soc. Greece, vol. 40, no. 2, pp. 666–675, 2007.

[62] K. G. Papke, "Nevada; Nevada Bureau of Mines and Geology, Bulletin 79," Reno, NV Mackay Sch. Mines/University Nevada, p. 32, 1972.

[63] R. de Gennaro, P. Cappelletti, G. Cerri, M. De Gennaro, M. Dondi, and A. Langella, "Zeolitic tuffs as raw materials for lightweight aggregates," Appl. Clay Sci., vol. 25, no. 1–2, pp. 71–81, 2004.

[64] M. Shaban and M. R. Abukhadra, "Geochemical evaluation and environmental application of Yemeni natural zeolite as sorbent for $Cd^{2+}$ from solution: kinetic modeling, equilibrium studies, and statistical optimization," Environ. Earth Sci., vol. 76, no. 8, pp. 1–16, 2017, doi: 10.1007/s12665-017-6636-3.

[65] A. Alshameri1, W. Xinghu, A. S. Dawood, C. Xin, ChunjieYan, and A. M. Assabri, "Characterization of Yemeni Natural Zeolite ( Al-Ahyuq Area ) and its Environment Applications : A Review," J. Ecol. Eng., vol. 20, no. 4, pp. 157–166, 2019.

[66] M. Albayrak and A. M. Ozgüner, "Geology and diagenesis of a zeolitic Foça tuff unit deposited in a Miocene phreatomagmatic lacustrine environment (western Anatolia)," Turkish J. Earth Sci., vol. 22, no. 4, pp. 611–631, 2013.

[67] S. Wang and Z. H. Zhu, "Characterisation and environmental application of an Australian natural zeolite for basic dye removal from aqueous solution," J. Hazard. Mater., vol. 136, no. 3, pp. 946–952, 2006.

[68] E. G. Beqiraj, F. Muller, and A. Beqiraj, "Mineralogical and Geochemical Characterization of Zeolites in Albanian Ophiolitic Plagiogranites," Bull. Geol. Soc. Greece, vol. 50, no. 4, pp. 1781–1788, 2016.